

X International Conference on Structural Dynamics, EURODYN 2017

Damage assessment of hollow core reinforced and prestressed concrete slabs subjected to blast loading

A.Maazoun^{ab}, J.Vantomme^a, S.Matthys^b

^aRoyal Military Academy, Civil and Materials Eng Dept, 30 av.de la renaissance, Brussels 1000, Belgium

^bGhent University, Magel Laboratory for Concrete Research, 904 Technologiepark-Zwijnaarde, Gent 9052, Belgium

Abstract

This paper presents an investigation of the deformations and damage modes, which occur in reinforced concrete (RC) or prestressed concrete (PC) hollow core slabs subjected to blast loads. This study focuses on four tests which have been performed on hollow core slabs with a compression layer, simply supported, subjected to explosions with different standoff distances for a constant charge weight. The paper discusses the numerical analysis carried out using the finite element software LS-DYNA. The results indicate that the appearance and growth of flexural cracks in concrete is delayed effectively by using prestressing. Moreover, prestressing decreases the deflection at mid-span of the tested hollow core slab and reduces the oscillation period due to the increase of the flexural stiffness and resistance of the hollow core slabs.

© 2017 The Authors. Published by Elsevier Ltd.

Peer-review under responsibility of the organizing committee of EURODYN 2017.

Keywords: Blast loading; Hollow core slab; Prestressed slab; Dynamic response; Failure mode

1. Introduction

Reinforced and prestressed concrete hollow core slabs are widely used for building and car parks applications. Most of the studies on hollow core slabs are focused on static load and fire resistance. Baran [1] tested five precast concrete hollow core units with concrete topping under flexural loading, in order to demonstrate that the concrete topping improves the flexural response of the panels. A layer of 50 mm thickness placed over the hollow core slabs shows an increase of the cracking moment and initial stiffness by 22% and 93% respectively. Shakhya et al. [2] investigated the response of precast prestressed concrete hollow core slabs under fire conditions, using two different types of aggregates (carbonate and siliceous). They conclude that hollow core slabs with carbonate aggregates exhibit higher fire resistance than those with siliceous aggregates, by up to 10%. The present study focuses on four tests which have been performed on hollow core slabs with a concrete topping subjected to explosions with different standoff for a constant charge weight. A numerical analysis is carried out and validated with experimental results.

2. Experimental program

2.1. Test Specimens

The slabs used in this study were 4 precast hollow cores slabs, with nominal dimensions 6 m length, 0.6 m width and 0.165 m thickness, two in reinforced and two in prestressed concrete, respectively designated RCHC and PCHC slabs (Fig. 1). The compressive cylinder strength of the concrete, $f_c=45\text{ N/mm}^2$, tensile strength, $f_{ct}=3.8\text{ N/mm}^2$, and modulus of elasticity, $E_c=36,300\text{ N/mm}^2$ were considered as per manufacturer's technical sheet. For RCHCS the main reinforcement is composed of 6 bars of 10 mm diameter. The reinforcement has a characteristic yield strength of $f_{yk}=500\text{ N/mm}^2$ and Young's modulus of $E_s=200,000\text{ N/mm}^2$. The PCHCS specimens contain six 2-wire pretensioned tendons of 7 mm diameter placed near the soffit and two 2-wire pretensioned tendons of 5mm diameter near the top of the slab. The characteristic tensile strength of the tendons $f_{yk}=1770\text{ N/mm}^2$ and the prestress force $F_p=259\text{ kN}$ were also considered as per manufacturer's technical sheet. Fig.1 shows the geometry and the section of the RCHC and PCHC slabs.

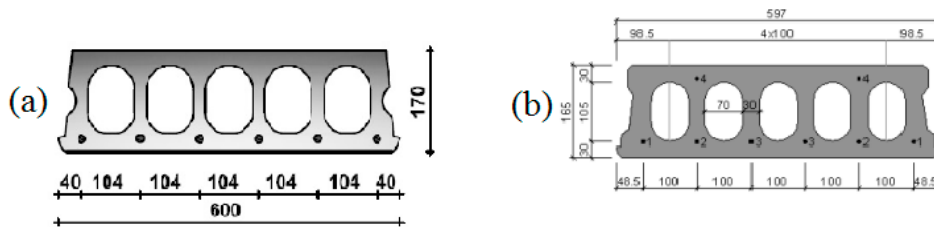


Fig. 1. (a) RCHC slab; (b) PCHC slab.

The top surface of the hollow core slabs are cleaned to remove any dust and debris before the cast of the compression layer. The steel used for the compression layer of the RCHC slab was a welded mesh of 5 mm diameter spaced at a distance of 150 mm and for the PCHC slab it was a welded mesh of 6 mm diameter. The thickness of the concrete cover was 50 mm, the compressive strength, tensile strength and Young's modulus of concrete were $f_c=30\text{ N/mm}^2$, $f_{ct}=2.9\text{ N/mm}^2$ and $E_c=32,800\text{ N/mm}^2$, respectively. The reinforcement had a characteristic yield strength of $f_{yk}=500\text{ N/mm}^2$ and Young's modulus of $E_s=200,000\text{ N/mm}^2$.

2.2. Experimental set up

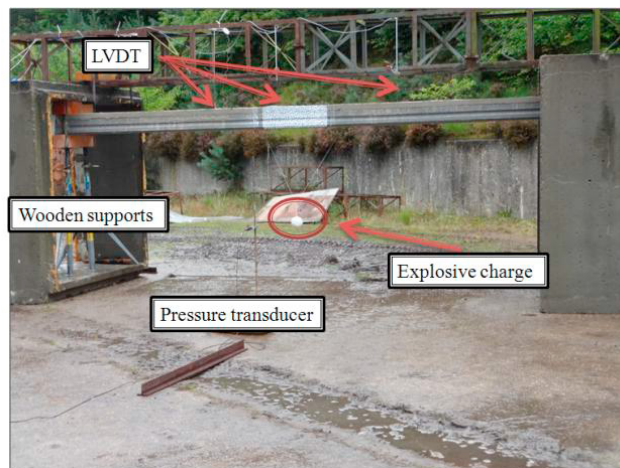


Fig. 2. Experimental set-up

Four tests have been performed, on two reinforced concrete hollow core slabs (RCHCS) and two prestressed concrete hollow core slabs (PCHCS), subjected to explosions with different standoff distances for a constant charge weight (Table 1). The slabs are simply supported at both sides by wooden pieces of 150 mm width, in order to allow small rotations of the slab ends. Linear Variable Displacement Transducers (LVDT) were used to measure the vertical displacement of the slab. All the LVDTs were fixed to the top side of the slab. Pressure Transducers are used on all the blast tests to record the pressure in the free air. Figure 2 shows the test set-up and the location of the instruments: three LVDTs placed at different positions along the length, a pressure transducer was placed at 2m from the explosive charge to measure the reflected pressure. In this work, a charge weight of 1.5 kg of C4 is suspended in the middle, underneath the slab at a variable height. Table 1 summarizes the testing program and shows the details of the experiment.

Table 1. Experimental details of the hollow core slabs and the explosive charge.

Test	Slab type	Length between supports (m)	Standoff distance (m)	Scaled distance (m/kg ^{1/3})	Explosive charge weight (kg)	Reflected pressure (MPa)	Reflected impulse (kPa.ms)
1	RCHC slab	5.4	1	0.8	1.5	9.19	927.5
2	RCHC slab	5.4	0.5	0.4	1.5	47.35	2496
3	PCHC slab	5.6	0.5	0.4	1.5	47.35	2496
4	PCHC slab	5.6	0.3	0.24	1.5	117.1	5596

3. Finite element analysis

3.1. Numerical model

A three-dimensional (3D) finite element model of the hollow core slab is developed and the analysis is performed using the LS-DYNA explicit solver [3]. An eight-node solid element with reduced integration scheme is used to model the concrete elements. A two-node beam element is used to model the reinforcement in the concrete, type Hughes-Liu with cross-section integration. The reinforcement elements are embedded within the concrete elements via the LS-DYNA command ‘constrained Lagrange in solid’. For blast studies due to the short duration and the high pressure of the explosion, a good interaction between concrete and steel is assumed [4]. Due to the symmetry of the specimens, and the time cost of the simulations, a quarter of the slab is considered. To present the prestressing force in the tendons a command ‘initial axial beam’ is used with a control command ‘dynamic relaxation’ to initialize the stresses and deformation in the model. The prestress force was applied to both initialization and transient analysis. For blast load modelling, the Lagrangian approach was used for applying the blast loads on the RC slab by means of ‘blast-load-enhanced’ keyword. It is the simplest approach and requires less time for analysis only the mass and coordinate of the explosive charge need to be defined. A schematic finite element detail for RCHC with a compression layer is shown in fig.3.

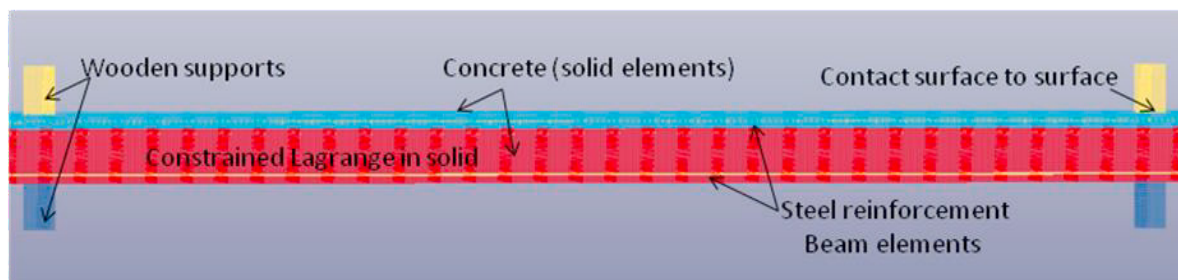


Fig.3. A schematic finite element detail for RCHC with a compression layer

3.2. Material constitutive models

For the concrete modelling, the Winfrith concrete model ‘mat-084’ was chosen. This material utilizes smeared cracking (pseudo cracking), depending on crack width and aggregate size [5]. The Winfrith model includes the strain rate effects and can predict the local and global response of concrete structures subject to accidental impact and blast loadings. The steel rebar and the tendons have been modelled using ‘mat-piecewise-linear-plasticity’. This elasto-plastic material model represents steel reinforcement behaviour, with plastic deformation, strain rate effects, and failure [5].

4. Results and discussion

4.1. Validation of the numerical results with the experimental data

Four scenarios are examined, the first scenario involves the use of a charge of 1.5 kg of C4 at a standoff distance of 1m suspended in the middle of the RCHC slab. The slab exhibited a global bending elastic behavior. Due to the steel reinforcement in the compression layer, the flexural stiffness of the slab increased and the specimen remained in the elastic deformation. Thin flexural cracks are observed on the top side of the slab. A maximum deflection of 26 mm was experimentally observed. Fig.4 shows the cracks marked after the test at the mid-span of the slab compared to the numerical model.

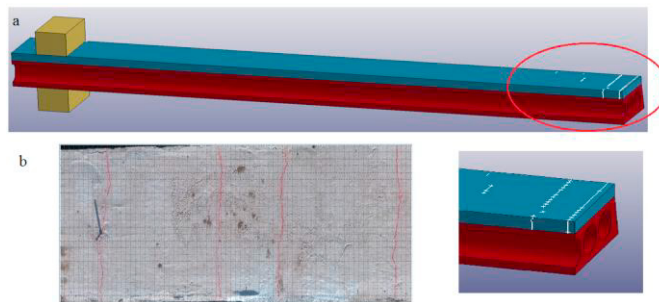


Fig. 4. (a) A quarter FE model of RCHC slab with a zoom in the middle part; (b) flexural cracks on the top side at the mid-span of the RCHC slab

For the second scenario, with a charge of 1.5 kg of C4 at a standoff distance of 0.5 m, the reflected pressure increased and the RCHC slab reached the plastic deformation. A significant deep crack was observed at the plastic hinge region of the slab. At the side faces of the slab a longitudinal crack was observed. The slab exceeded its elastic limit and reached a maximum deflection of 65.5 mm. Fig.5 shows the comparison of the distribution of the cracks on the top side and the longitudinal cracks on the side face of the slab with the numerical model.

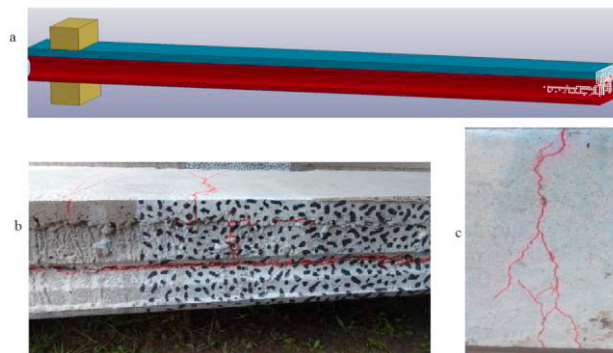


Fig. 5. (a) A quarter FE model of RCHCS; (b) longitudinal crack on the front side of the slab; (c) deep flexural crack at the mid-span of the slab

In the third scenario, a PCHC slab is tested at the same standoff distance 0.5 m as the second scenario. A maximum deflection of 57.22 mm was experimentally observed. Hence, the slab showed less deflection at mid-span of the slab than the RCHC slab. In this case, the two tendons in the top layer of the PRHC slab increase the bending stiffness of the slab and the shear capacity near the hollow core. It should be noted that the strength of the prestressing tendons is larger than the strength of ordinary reinforcement steel. Thin flexural cracks are observed on the top side of the slab with a longitudinal crack at the sides of the slab as shown in Fig. 6.

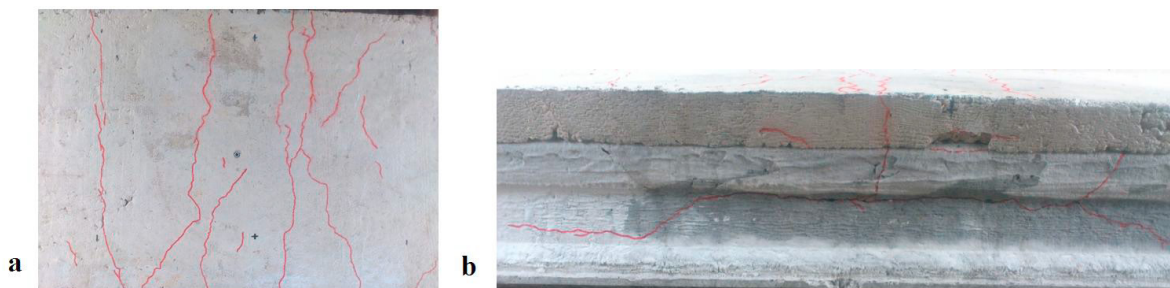


Fig. 6. (a) flexural cracks at the mid-span of the slab; (b) longitudinal crack on the side of the slab.

For the last scenario, 1.5kg of C4 has been suspended at the middle of the PCHC slab with a standoff distance 0.3 m. The reflected pressure increases the blast wave. A debonding between the compression layer and PCHC slab was observed, and slippage occurred at the interface of the two concrete components in the horizontal direction as shown in Fig. 7. When the slab vibrates, a horizontal shear stress appears between the interface of the overlay and the hollow core slab. According to Eurocode, the interface shear strength between the compression layer and the PCHC slab depends on the surface roughness of the slab and the concrete strength [6]. The surface was smooth, which provides a weak friction with the concrete topping. Also, it should be noted that the blast wave impacting the specimens is partially reflected and partially propagates through the slab cross-section, generating normal stress in addition to the aforementioned shear stresses. In fact, the compressive stress wave travelled across the hollow core slab to the concrete topping, and is reflected back as a tensile wave. This tensile wave can be much higher than the allowable interface normal stress between the hollow core slab and the concrete topping, and enhances the debonding problem.

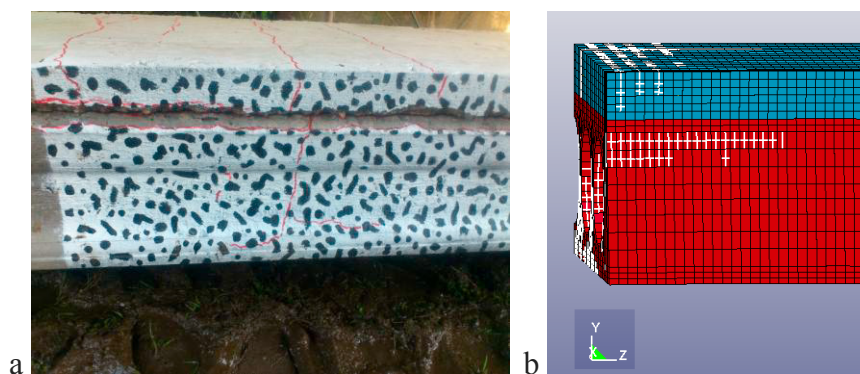


Fig. 7. (a) debonding between the overlay and the PCHC slab; (b) a quarter FE model of PCHC slab.

4.2. Damage aspect of RCHC and PCHC slabs subjected to blast loading

To evaluate the damage observed on the slabs, two parameters should be taken into account. The first parameter is the support rotation defined as the angle made between a straight segment and the plastic hinge. The second parameter is the maximum deflection recorded at the mid-span of the slabs. Table 3 reports these two parameters, as well as the failure modes of the slabs after the explosion.

Table 3. Damage assessment of RCHC and PCHC slabs.

Test	Type of the slabs	Max deflection exp(mm)	Max deflection num (mm)	Support rotation Θ (°)	Damage level	Failure modes
1	RCHC slab	26	32	0.55	Superficial damage	Thin flexural cracks on the top of the slab
2	RCHC slab	65.5	68	1.38	Moderate damage	Deep and wide flexural cracks on the top of the slab with longitudinal crack on the sides of the slab
3	PCHC slab	57.22	57.4	1.17	Superficial damage	Flexural cracks on the top of the slab with a thin longitudinal crack on the sides of the slab
4	PCHC slab	73.4	74	1.5	Moderate damage	Flexural cracks on the compression layer, longitudinal cracks on the sides of the slab debonding between the compression layer

5. Conclusions

This study presents the experimental and numerical results of RCHC and PCHC slabs with a compression layer, simply-supported, under blast loading. Numerical analysis show a good agreement with the experimental results for the maximum deflection at the mid-span of the slabs. The numerical model also gave a good prediction of the observed cracking. The effects of prestressing delayed the appearance and the growth of flexural cracks in the concrete and lead to a smaller deflection at the mid-span of the PCHC slab compared to RCHC slab. The dynamic response of the PCHC slab is stiffer than the RCHC slab (reducing the maximum deflection and the oscillation period). The prestressing increases the flexural resistance capacity of the hollow core slabs. Proper analysis and design are necessary to determine the optimal prestressing levels to enhance the blast loading capacities of RC slabs. Further analysis is needed on devices to strengthen the interfacial connection and thus to ensure proper shear transfer between the overlay and the hollow core slab to reach a complete composite action and avoid the debonding.

Acknowledgements

The authors thank the companies ECHO and Douterloigne for delivery of specimens slabs.

References

- [1] E. Baran, Effects of cast-in-place concrete topping on flexural response of precast concrete hollow-core slabs, *Engineering Structures* 98 (2015) 109-117.
- [2] A.M.Shakya, V.K.R. Kodur, Response of precast prestressed concrete hollow core slabs under fire conditions, *Engineering Structures* 85 (2015) 126-138.
- [3] A. Maazoun, S. Matthys, and J. Vantomme, Numerical Prediction of the Dynamic Response of Reinforced Concrete Hollow Core Slabs under Blast Loading ,11th European LS-DYNA conference , 2017.
- [4] L. Schwer, Modeling rebar : The forgotten sister in reinforced concrete modeling, 13th International LS-DYNA® Users Conference, 2014.
- [5] LS-DYNA KEYWORD USER'S MANUEL,(2016).
- [6] CEN. Eurocode 2: design of concrete structures – Part 1-1: general rules and rules for buildings: EN 1992-1-1. Brussels: European Committee for Standardization,(2005).